Journal of Experimental Botany, Vol. 70, No. 10 pp. 2773–2786, 2019
doi:10.1093/jxb/erz083 Advance Access Publication 6 March 2019
This paper is available online free of all access charges (see https://academic.oup.com/jxb/pages/openaccess for further details)

RESEARCH PAPER

Knockdown of glycine decarboxylase complex alters photorespiratory carbon isotope fractionation in *Oryza sativa* leaves

Rita Giuliani[1], Shanta Karki[2], Sarah Covshoff[3], Hsiang-Chun Lin[2], Robert A. Coe[2], Nuria K. Koteyeva[4], W. Paul Quick[2,5], Susanne von Caemmerer[6], Robert T. Furbank[6], Julian M. Hibberd[3], Gerald E. Edwards[1] and Asaph B. Cousins[1,*]

[1] School of Biological Sciences, Molecular Plant Sciences, Washington State University, Pullman, WA 99164, USA
[2] C_4 Rice Center, International Rice Research Institute (IRRI), Los Baños, Philippines
[3] Department of Plant Sciences, University of Cambridge, Cambridge CB2 3EA, UK
[4] Laboratory of Anatomy and Morphology, V.L. Komarov Botanical Institute of the Russian Academy of Sciences, Prof. Popov Street 2, 197376, St. Petersburg, Russia
[5] Department of Animal and Plant Sciences, University of Sheffield, Sheffield S10 2TN, UK
[6] Division of Plant Sciences, Research School of Biology, The Australian National University, Canberra ACT 0200, Australia

* Correspondence: acousins@wsu.edu

Received 23 October 2018; Editorial decision 12 February 2019; Accepted 12 February 2019

Editor: Christine Foyer, Leeds University, UK

Abstract

The influence of reduced glycine decarboxylase complex (GDC) activity on leaf atmosphere CO_2 and $^{13}CO_2$ exchange was tested in transgenic *Oryza sativa* with the GDC H-subunit knocked down in leaf mesophyll cells. Leaf measurements on transgenic *gdch* knockdown and wild-type plants were carried out in the light under photorespiratory and low photorespiratory conditions (*i.e.* 18.4 kPa and 1.84 kPa atmospheric O_2 partial pressure, respectively), and in the dark. Under approximately current ambient O_2 partial pressure (18.4 kPa pO_2), the *gdch* knockdown plants showed an expected photorespiratory-deficient phenotype, with lower leaf net CO_2 assimilation rates (A) than the wild-type. Additionally, under these conditions, the *gdch* knockdown plants had greater leaf net discrimination against $^{13}CO_2$ (Δ_o) than the wild-type. This difference in Δ_o was in part due to lower ^{13}C photorespiratory fractionation (f) ascribed to alternative decarboxylation of photorespiratory intermediates. Furthermore, the leaf dark respiration rate (R_d) was enhanced and the $^{13}CO_2$ composition of respired CO_2 ($\delta^{13}C_{Rd}$) showed a tendency to be more depleted in the *gdch* knockdown plants. These changes in R_d and $\delta^{13}C_{Rd}$ were due to the amount and carbon isotopic composition of substrates available for dark respiration. These results demonstrate that impairment of the photorespiratory pathway affects leaf $^{13}CO_2$ exchange, particularly the ^{13}C decarboxylation fractionation associated with photorespiration.

Keywords: ^{13}C discrimination, C_4 photosynthesis, CO_2 exchange, GDC knockdown, leaf dark respiration, photorespiration, rice.

Introduction

In C_3 plants, Rubisco operates in the leaf mesophyll cells, where CO_2 and O_2 compete to react with ribulose-1,5-bisphosphate (RuBP). The carboxylation of RuBP results in the formation of two molecules of 3-phosphoglycerate (3-PGA) that are integrated into the Calvin–Benson cycle. Alternatively, the oxygenation of RuBP produces one molecule of 3-PGA and one

2-phosphoglycolate (2-PG). The 2-PG is primarily recycled via photorespiration through a complex and energy-consuming set of reactions, which spans the chloroplasts, cytosol, peroxisomes, and mitochondria (Bauwe *et al.*, 2010; Betti *et al.*, 2016). By scavenging 2-PG, photorespiration removes a strong inhibitor of enzymes in photosynthetic carbon metabolism (Anderson, 1971; Kelly and Latzko, 1976; Peterhansel *et al.*, 2013*b*; Walker *et al.*, 2016) and recovers up to one molecule of 3-PGA for every two molecules of 2-PG. Nevertheless, a minimum of one out of four 2-PG carbon atoms is released as CO_2 by the glycine decarboxylase complex (GDC) and can be lost by the plant (Bauwe, 2018).

The GDC is an atypical mitochondrial four-protein system, comprised of three enzymes (P-, T-, and L-protein) and the H-protein, which is a small lipoylated protein (Somerville and Ogren, 1982; Douce *et al.*, 2001; Bauwe, 2018). GDC plays a critical role in the photorespiratory cycle by catalyzing the conversion of two molecules of glycine into serine and one molecule of CO_2 and NH_3 (Somerville, 2001; Maurino and Peterhansel, 2010). However, in the absence of the H component, the GDC cannot oxidize glycine (Douce *et al.*, 2001; Parys and Jastrzębski, 2008), which can accumulate. In C_3 plants, the impaired activity of the H-subunit leads to a knockdown (KD) of GDC activity and a photorespiratory phenotype (Ewald *et al.*, 2007). Plants with reduced GDC activity typically have lower rates of leaf photosynthesis, a depletion of Calvin cycle metabolites, an impairment of photorespiratory nitrogen re-assimilation, and the accumulation of photorespiratory metabolites (*e.g.* glycine) under current ambient CO_2 and O_2 partial pressures (Wingler *et al.*, 2000; Timm and Bauwe, 2013; Lin *et al.*, 2016).

This buildup of leaf photorespiratory metabolites can have a negative feedback effect on Calvin cycle activity. For example, glyoxylate produced by glycolate oxidation negatively impacts on the activation state of Rubisco (Wingler *et al.*, 1999; Peterhansel *et al.*, 2010). Additionally, disruption of the photorespiratory pathway may lead to alternative decarboxylation reactions of accumulated pools of photorespiratory intermediates, such as glyoxylate and hydroxypyruvate in the peroxysomes (Wingler *et al.*, 1999, 2000; Tcherkez, 2006; Peterhansel *et al.*, 2010), and an increase in the ratio of moles of photorespiratory CO_2 released per mole of O_2 reacting with RuBP (α; Cousins *et al.*, 2008, 2011; Walker and Cousins, 2013; Timm *et al.*, 2018). Furthermore, the accumulation of photorespiratory intermediates could also affect the rates of leaf CO_2 evolved in the dark (R_d, μmol CO_2 m^{-2} s^{-1}) and the ^{13}C composition of R_d ($\delta^{13}C_{Rd}$, ‰) (Ghashghaie *et al.*, 2003; Tcherkez *et al.*, 2003).

The multiple leaf metabolic reactions simultaneously consuming and releasing CO_2 in the light make it difficult to determine how changes in photorespiration affect rates of leaf net CO_2 assimilation (A), mesophyll CO_2 conductance (g_m), refixation of (photo)respired CO_2, and mitochondrial non-photorespiratory respiration rates (R_L). However, photosynthesizing leaves discriminate against ^{13}C during CO_2 diffusion from the atmosphere to the chloroplast stroma (through both the air and liquid phases), and during carboxylation, photorespiration, and mitochondrial non-photorespiratory respiration processes, with a specific ^{13}C fractionation for each diffusional or biochemical step (Evans *et al.*, 1986). The observed leaf net discrimination against ^{13}C in the light (Δ_o, ‰) can be modeled with four ^{13}C fractionation terms (‰): Δ_i, which accounts for the ^{13}C discrimination during CO_2 diffusion from the atmosphere to the intercellular air space and for the Rubisco ^{13}C fractionation (~29‰, Ubierna and Farquhar, 2014; von Caemmerer *et al.*, 2014); Δ_{gm}, which accounts for the ^{13}C discrimination during CO_2 diffusion in the liquid phase to chloroplast stroma and depends on the magnitude of g_m; and Δ_f and Δ_e which are associated with photorespiration and mitochondrial non-photorespiratory respiration activity, respectively (von Caemmerer and Evans, 1991; Flexas *et al.*, 2008; Tazoe *et al.*, 2011; Evans and von Caemmerer, 2013). Δ_f is primarily attributed to the glycine–serine reaction catalyzed by GDC, which releases CO_2 depleted in ^{13}C compared with substrate and tends to decrease Δ_o (Farquhar *et al.*, 1982; Ghashghaie *et al.*, 2003; Lanigan *et al.*, 2008). In contrast, Δ_e may increase or decrease Δ_o in relation to the difference between ^{13}C composition (‰) of CO_2 entering the leaf chamber during measurements and in the plant growth chamber (Gillon and Griffiths, 1997; Ghashghaie *et al.*, 2003).

The photorespiratory fractionation (f, ‰) estimated *in vivo* in multiple C_3 species ranges between 8‰ and 16.2‰ relative to photosynthetic products (Ghashghaie *et al.*, 2003; Evans and von Caemmerer, 2013), with 11‰ predicted from the theory (Tcherkez, 2006). However, under photorespiratory conditions, when Rubisco oxygenation exceeds the capacity of the photorespiratory recycling of 2-PG or in the presence of disruption of the photorespiratory pathway, Δ_f and f may vary due to changes in α associated with alternative decarboxylation of photorespiratory intermediates (Cousins *et al.*, 2008, 2011; Walker and Cousins, 2013). Alternative photorespiratory bypasses may occur in the chloroplasts (*e.g.* glyoxylate may be enzymatically reduced back to glycolate or further oxidized to CO_2, but with no RuBP regenerated; see Kebeish *et al.*, 2007), peroxysomes (non-enzymatic decarboxylation of glyoxylate to formate using H_2O_2 as oxidizing agent may lead to formation of serine; catalase may be also involved as reported in Wingler *et al.*, 1999), mitochondria (enzymatic oxidation of glycolate to glyoxylate with release of CO_2 and synthesis of glycine; see Niessen *et al.*, 2007), and cytosol (enzymatic reduction of hydroxypiruvate to glycerate; see Timm *et al.*, 2008).

The aim of the present study was to test how changes in carbon flux through the photorespiratory pathway influenced leaf CO_2 and $^{13}CO_2$ isotope exchange, both in the light and in the dark, in transgenic plants of *Oryza sativa* with the GDC H-subunit KD in mesophyll cells. Both *gdch*-KD and wild-type (WT) plants were grown under low photorespiratory conditions (atmospheric CO_2 partial pressure of 184.2 Pa) to minimize any pleiotropic effects. In the light, measurements of leaf–atmosphere CO_2 and stable carbon isotope exchange were performed under low photorespiratory and photorespiratory conditions (atmospheric O_2 partial pressure of 1.84 kPa or 18.4 kPa, respectively, and CO_2 partial pressure of 27.6 Pa). The disruption of the photorespiratory pathway in the *gdch*-KD plants was characterized by leaf photosynthetic traits, Δ_o, Δ_f, f, α, R_d, and $\delta^{13}C_{Rd}$, compared with the WT.

Materials and methods

Plant material

Generation of GDC-H knockdown transgenic rice lines

The generation and the characterization of three *Oryza sativa gdch*-KD transgenic lines, including *gdch*-38, was previously described by Lin *et al.* (2016). Line *gdch*-38 was selected for analysis in the present study since in Lin *et al.* (2016) it had shown a more consistent photorespiratory-deficient phenotype under different O_2:CO_2 growing and measuring conditions compared with the other two *gdch*-KD lines. Untransformed *O. sativa* cv. IR64 line A009 (WT) was used as negative control for comparison with the *gdch*-KD line.

Plant growth conditions

Two batches of 10 transgenic *gdch*-38 line (T_4 generation) and 10 WT plants of *O. sativa* cv. IR64 were grown consecutively in a controlled-environment growth chamber (G_{ch}; Bigfoot series, BioChambers Inc., Winnipeg, MB, Canada) at the School of Biological Sciences at Washington State University, Pullman, WA (USA). All plants were individually grown in 4 liter free drainage pots; soil, irrigation, and fertilization were as in Giuliani *et al.* (2013).

The daily photoperiod was 14 h, from 8.00 h to 22.00 h standard time. Light was provided by F54T5/841HO Fluorescent 4100 K and 40 W halogen incandescent bulbs (Philips) and was supplied in a bell-shaped pattern; that is, with increasing photosynthetic photon flux density (PPFD) during the first 2 h, a maximum PPFD of 600 µmol photons m^{-2} s^{-1} incident on the plant canopy for 10 h, and decreasing PPFD in the last 2 h. Air temperature (t_{air}) was set at 22 °C in the dark period; after switching on the light, t_{air} tracked the PPFD pattern; that is, it ramped during the first 2 h from 22 °C to 26 °C, then 26 °C for 10 h, and decreased to 22 °C in the last 2 h photoperiod. Air relative humidity was maintained at ~70%, corresponding to a maximum air vapor pressure deficit (VPD) of ~1.6 kPa. During the light period, the CO_2 partial pressure (pCO_2) in the G_{ch} atmosphere was elevated to 184.2 Pa (2000 µmol mol^{-1}). The ^{13}C composition of the atmospheric CO_2 during the light period ($\delta^{13}C_{Gch}$) was −41.6‰ and −30.6‰ for the first and second batch of grown plants, respectively. The $\delta^{13}C_{Gch}$ was determined as described in Supplementary Methods S1 at *JXB* online, and was a proxy of the ^{13}C composition of the CO_2 in the tank used (during the second plant growing cycle a new tank was needed and no tank with $^{13}CO_2$ composition comparable with the previous one was available).

Leaf biochemical analysis

Protein content

Protein immunoblot analysis was performed to determine the leaf abundance of GDC H-, P-, and T-subunits in fully expanded leaves of 4- to 5-week-old transgenic *gdch*-KD and WT plants. For each genotype, two separate protein extractions were performed, each one using the leaf tissue collected from two plants, according to Koteyeva *et al.* (2015). Protein concentration was determined for each extract with an RC DC protein quantification kit (Bio-Rad, Hercules, CA, USA) and 20 µg of protein per extract were separated by 10% (w/v) SDS–PAGE for the GDC P-subunit or 15% (w/v) for GDC H- and T-subunits. Proteins were then transferred to a nitrocellulose membrane and immunoblots (n=2 for both *gdch*-KD and WT) were performed according to Koteyeva *et al.* (2015) with primary antibodies for anti-*Pisum sativum* L. GDC H-, P-, and T-subunits (1:10 000) raised in rabbit (courtesy of Dr D. Oliver, Iowa State University). The L-subunit was not detected because antibodies were unavailable. The band intensities were quantified with ImageJ 1.37 software (NIH, USA).

Malate content

The leaf portions used for photosynthesis analysis in *gdch*-KD and WT plants (n=5) were sampled immediately after the leaf–atmosphere gas exchange measurements and frozen in liquid N_2. Malate content per unit leaf surface area (mmol malate m^{-2}) was then determined with a spectrophotometry-based assay as described by Hatch (1979), with modifications by Edwards *et al.* (1982).

Leaf physiological analysis

Coupled measurements of leaf–atmosphere CO_2, H_2O, and $^{13}CO_2$ exchange

Measurements were performed in Pullman, WA, USA with a mean atmospheric pressure of 92.1 kPa. Two LI-6400XT portable gas analyzers (LI-COR Biosciences, Lincoln, NE, USA; detecting $^{12}CO_2$) operating as open systems were coupled to a tunable diode laser absorption spectroscope, which detects $^{12}CO_2$ and $^{13}CO_2$ isotopologs (TDLAS model TGA200A, Campbell Scientific, Inc., Logan, UT, USA; Bowling *et al.*, 2003; Barbour *et al.*, 2007; Ubierna *et al.*, 2011; Stutz *et al.*, 2014; Sun *et al.*, 2014). Additional technical information on the system setup are available in Supplementary Methods S2.

For the leaf photosynthesis measurements, each LI-COR was equipped with a 2×3 cm leaf chamber (L_{ch}) assembled with an LED light source (6400-02B; LI-COR Biosciences). Alternatively, leaf dark respiration measurements were performed using an 8×10 cm custom-built L_{ch} having an adaxial glass window, and with a volume of ~100 cm^3 (Barbour *et al.*, 2007, based on Sharkey *et al.*, 1985). The chamber had a hollowed stainless steel frame sealed with a closed-cell foam gasket and was connected to a circulating water bath for temperature control in the lumen. Before dark respiration measurements, the leaf portions included in the L_{ch} were exposed to the light, which was supplied by a LI-COR 6400-18 light source placed adjacent to the glass window.

Protocol for coupled measurements of leaf–atmosphere CO_2, H_2O, and $^{13}CO_2$ exchange

The mid to distal portions of two fully expanded leaves from the same stem on 4- to 5-week-old plants (n=4 for *gdch*-KD; n=5 for WT) grown under $\delta^{13}C_{Gch}$ of −41.6‰ were used for leaf photosynthetic measurements. The leaves were positioned to cover the 6 cm^2 L_{ch} section area. Measurements were taken from 10.00 h until 16.00 h standard time under an O_2 partial pressure (pO_2) of 18.4 kPa (approximately the current atmospheric pO_2) and 1.84 kPa, pCO_2 (C_a) of 27.6 Pa, and ^{13}C composition of CO_2 (from a pressurized tank) entering the L_{ch} (δ_{in}) of −48.0‰. PPFD was set at 1500 µmol photons m^{-2} s^{-1}, leaf temperature (t_{leaf}) at 25 °C, and leaf to air VPD was kept between 1.0 kPa and 1.5 kPa. The airflow rate through the LI-COR system was 300 µmol s^{-1} (~0.48 l min^{-1}). In particular, a C_a below current ambient pCO_2 (which was ~37 Pa) was chosen to amplify, under a pO_2 of 18.4 kPa, the signals of the photorespiratory-deficient phenotype in the *gdch*-KD plants compared with the WT.

Under each experimental O_2 condition, leaf portions were acclimated for ~30 min and data were recorded for ~30–40 min. The rate of net CO_2 assimilation per unit (one side) leaf surface area (A, µmol CO_2 m^{-2} s^{-1}), stomatal conductance to CO_2 diffusion (g_{sC}, µmol CO_2 m^{-2} s^{-1} Pa^{-1}), intercellular pCO_2 (C_i, Pa), and the ratio C_i/C_a were determined.

For leaf dark respiration measurements, *gdch*-KD and WT plants (n=4) grown at a $\delta^{13}C_{Gch}$ of both −41.6‰ and −30.6‰ were used. Two plants per day (one *gdch*-KD and one WT) were taken out of the G_{ch} at 9.30 h standard time and the mid to distal portions of 8–9 fully expanded leaves, similar to those used for the photosynthetic analysis, were enclosed in the custom-built L_{ch} to cover the section area of ~76 cm^2. Leaf portions were first exposed to a PPFD of 750 µmol photons m^{-2} s^{-1} for 20 min, 500 µmol photons m^{-2} s^{-1} for 15 min (at t_{leaf} of 25 °C), and 100 µmol photons m^{-2} s^{-1} for 5 min (at t_{leaf} of 30 °C). Measurements were taken under a pO_2 of 1.84 kPa or 18.4 kPa for plants grown at a $\delta^{13}C_{Gch}$ of −41.6‰ or −30.6‰, respectively. C_a was set at 35.0 Pa, and the airflow rate through the LI-COR was changed from 700 µmol s^{-1} to 500 $µmol^{-1}$, and from 500 µmol s^{-1} to 350 µmol s^{-1} tracking the decreasing PPFD. A CO_2 cartridge from a set of cartridges with $\delta^{13}C$ from −6.2‰ to −4.8‰ was used, one per day, as CO_2 source (the mean δ_{in} for all experimental conditions is shown in Supplementary Table S1). The different (higher) $\delta^{13}CO_2$ composition entering the L_{ch} with respect to the G_{ch} (−41.6‰) was chosen to have the leaf carbon assimilates

produced in the L_{ch} with dissimilar (higher) $\delta^{13}C$ signatures compared with those previously produced in the G_{ch}. After 40 min of leaf light exposure, darkness was imposed in the L_{ch}. Leaf CO_2 evolution was measured at a pO_2 of 18.4 kPa and t_{leaf} of 30 °C for 195 min to determine the dynamics of the dark respiration rate per unit (one side) of leaf surface area (R_d, μmol CO_2 m^{-2} s^{-1}) and corresponding $\delta^{13}C$ ($\delta^{13}C_{Rd}$, ‰). The t_{leaf} was set at 30 °C to enhance the precision of the dark measurements. Additionally, three plants (n=3) of the *gdch*-KD line and of the WT were taken out of the growth chamber at 12.00 h standard time 3 d after their use for measurements, and darkened at 25 °C for 24 h. Subsequently, leaf dark CO_2 evolution was measured at a t_{leaf} of 30 °C and a pO_2 of 18.4 kPa to determine $R_{d(24h)}$ (μmol CO_2 m^{-2} s^{-1}) and $\delta^{13}C_{Rd(24h)}$ (‰). The blade portions used for dark measurements on WT and *gdch*-KD plants were sampled and dried in a ventilated oven at 55 °C for 48 h to determine leaf dry mass per (one side) unit of leaf surface area (LMA, g m^{-2}).

For each *gdch*-KD and WT plant used for leaf photosynthesis measurements, the ^{13}C signature of leaf dry matter ($\delta^{13}C_{dm}$, ‰) and leaf total N content as a fraction (%) of dry matter were determined as described in Supplementary Methods S3, and the leaf total N content per unit leaf surface area (g m^{-2}) was calculated. The descriptions, values, and units of abbreviations and symbols are listed in Table 1.

Leaf net $^{13}CO_2$ discrimination in the light and mesophyll conductance to CO_2 diffusion

The observed leaf net discrimination against $^{13}CO_2$ in the light (Δ_o, ‰) was calculated by mass balance from the TDLAS measurements according to Evans *et al.* (1986). Under photorespiratory conditions (18.4 kPa pO_2), the $^{13}CO_2$ fractionation for photorespiration (f, ‰) in the *gdch*-KD plants was calculated based on Evans and von Caemmerer (2013). Briefly, the value of f was determined by modeling the leaf net discrimination against $^{13}CO_2$ (Δ_o) as a function of the ^{13}C discrimination fractions associated with CO_2 diffusion from the atmosphere to the intercellular air space and with carboxylation (Δ_i), with CO_2 diffusion in liquid phase to chloroplast stroma (Δ_{gm}), mitochondrial non-photorespiratory respiration (Δ_e), and photorespiration (Δ_f). The equation $\Delta_o=\Delta_i-\Delta_{gm}-\Delta_f-\Delta_e$ can be rearranged so that $\Delta_f=\Delta_i-\Delta_o-\Delta_{gm}-\Delta_e$ and f can be estimated by substituting Δ_f with $\Delta_f = \frac{1+t}{1-t}\left(f\frac{\Gamma^*}{C_a}\right)$ to get $\frac{1+t}{1-t}\left(f\frac{\Gamma^*}{C_a}\right) = \Delta_i-\Delta_o-\Delta_{gm}-\Delta_e$. An f value of 16.2‰ was taken from Evans and von Caemmerer (2013) and assumed for WT plants. The input parameters needed to calculate f include the leaf mitochondrial respiration rate in the light (R_L, μmol CO_2 m^{-2} s^{-1}), the CO_2 compensation point in the absence of mitochondrial non-photorespiratory respiration (Γ^*, μmol mol^{-1}), and mesophyll CO_2 conductance (g_m, mol CO_2 m^{-2} s^{-1}). Values of R_L at a t_{leaf} of 25 °C were modeled for both genotypes from the corresponding R_d at 30 °C after 3 h in the dark [$R_{d(3h)}$, μmol CO_2 m^{-2} s^{-1}] following leaf photosynthesis under atmospheric pO_2 of 18.4 kPa using the temperature response function in Bernacchi *et al.* (2001). The Γ^* was modeled based on von Caemmerer (2000), as described in Supplementary Methods S4, and was significantly different (P<0.05) between WT and *gdch*-KD plants, 45.0±1.7 SE (n=4) μmol mol^{-1} and 53.3±0.6 SE (n=3) μmol mol^{-1}, respectively. Finally, g_m was estimated based on leaf–atmosphere CO_2 and $^{13}CO_2$ exchange data, according to Evans and von Caemmerer (2013). Specifically, ^{13}C-based g_m was calculated in the *gdch*-KD and WT plants at 1.84 kPa pO_2, but only in WT plants under 18.4 kPa pO_2, using an f value of 16.2‰. The ^{13}C-based g_m cannot be calculated in *gdch*-KD plants at 18.4 kPa pO_2 because g_m and f are not independent variables in the applied procedure. Therefore, at 18.4 kPa, the g_m values of *gdch*-KD plants were set the same as for the WT. This assumes that the ^{13}C-based g_m integrates the within-leaf resistances affecting CO_2 movement across the cell wall, plasma membrane, and the chloroplast membranes, and that this cumulative resistance does not differ between *gdch*-KD and WT plants. This assumption is supported by the fact that the ^{18}O-based g_m, which was determined by analysis of leaf–atmosphere ^{18}O exchange according to Ubierna *et al.* (2017), Kolbe and Cousins (2018), and Sonawane and Cousins (2019), was not significantly different between the *gdch*-KD and WT plants at 18.4 kPa pO_2 (Supplementary Table S2). The ^{18}O-based g_m is not strictly associated with the biochemistry of photosynthesis as is the ^{13}C-based g_m and therefore cannot be used to estimate f. The values of ^{13}C-based g_m for *gdch*-KD and WT plants at each pO_2 were used to calculate the corresponding pCO_2 in the chloroplasts (C_c, Pa) by applying Fick's first law.

The Γ^* was defined in terms of Rubisco kinetic properties according to Jordan and Ogren (1984), and the estimate of CO_2 released per O_2 reacting with RuBP (α) was determined for the *gdch*-KD plants versus α set equal to 0.5 in the WT as described in Supplementary Methods S5. A sensitivity analysis for the dependency of f on Γ^* and α is also described in Supplementary Methods S5.

^{13}C composition of leaf dark-evolved CO_2 and contributions of leaf chamber and growth chamber assimilates to substrates feeding leaf dark respiration

The ^{13}C composition of the dark-evolved CO_2 determining R_d ($\delta^{13}C_{Rd}$, ‰) was calculated according to Barbour *et al.* (2007) as described by Evans *et al.* (1986).

The substrates feeding leaf dark respiration were from carbon assimilates produced in the L_{ch} and in the G_{ch}. Given $\delta^{13}C_{Rd(i)}$ as the mean values of $\delta^{13}C$ for dark-evolved CO_2 at time i from light–dark transition, the fractional contribution of L_{ch} assimilates to $\delta^{13}C_{Rd(i)}$ ($^{\delta Rd}L_{ch\_substr(i)}$, ‰/‰) was calculated for *gdch*-KD and WT plant types after leaf photosynthesis under both O_2 levels as

$$ {}^{\delta Rd}L_{ch\_substr(i)} = \frac{(\delta^{13}C_{Rd(i)} - \delta^{13}C_{Rd(24h)})}{(\delta^{13}C_{Lch\_Ph} - \delta^{13}C_{Rd(24h)})} \quad (1) $$

where $\delta^{13}C_{Rd(i)}$ was determined by steps of 3 min over 195 min in the dark; $\delta^{13}C_{Rd(24h)}$ is the mean $\delta^{13}C_{Rd}$ after 24 h in the dark as shown in Supplementary Table S1; and $\delta^{13}C_{Lch\_Ph}$ (‰) is the representative $\delta^{13}C$ of *gdch*-KD or WT carbon assimilates produced in the L_{ch} at a pO_2 of 1.84 kPa or 18.4 kPa before the light–dark transition (values are shown in Supplementary Table S1). The assumptions underlying Equation 1 and the calculation of $\delta^{13}C_{Lch\_Ph}$ are reported in Supplementary Methods S6.

Based on the total fractional contributions of L_{ch} and G_{ch} carbon assimilates to $\delta^{13}C_{Rd}$ equal to 1.0, the complementing fractional contribution of G_{ch} assimilates to $\delta^{13}C_{Rd(i)}$ [$^{\delta Rd}G_{ch\_substr(i)}$, ‰/‰] was calculated for both plant types after leaf photosynthesis under both O_2 levels as

$$ {}^{\delta Rd}G_{ch\_substr(i)} = 1 - {}^{\delta Rd}L_{ch\_substr(i)} \quad (2) $$

In addition, to make a combined analysis of the data collected in the two O_2 experimental conditions possible, the $\delta^{13}C_{Rd}$ generated from plants grown at the more depleted $\delta^{13}C_{Gch}$ were edited to cancel out the bias in the $\delta^{13}C_{Gch}$ effect on $\delta^{13}C_{Rd}$ with respect to the other batch of plants. In particular, the $\delta^{13}C_{Rd}$ following leaf photosynthesis at the lower O_2 experimental level were edited through the procedure described in Supplementary Methods S7.

Leaf CO_2 compensation points in the presence of R_L

Leaf–atmosphere gas exchange measurements were taken with an LI-6400XT portable gas analyzer equipped with the 2×3 cm L_{ch} on *gdch*-KD and WT plants (n=4) at a PPFD of 1500 μmol photons m^{-2} s^{-1}, t_{leaf} of 25 °C, leaf to air VPD between 1.0 kPa and 1.5 kPa, C_a decreasing from 35.0 Pa to 3.7 Pa, and at a pO_2 of 1.84 kPa or 18.4 kPa. For each leaf, a least square regression analysis of the response of A (μmol CO_2 m^{-2} s^{-1}) to C_i (Pa) was applied to the initial slope (for C_i≤9.2 Pa) to determine the CO_2 compensation point in the presence of R_L (Γ, Pa).

Statistical analysis

Statistical analyses were performed using SAS version 9.4 (SAS Institute, Cary, NC, USA). A linear mixed effects model (PROC MIXED) was used with plant type (*gdch*-KD and WT) and O_2 level (pO_2 of 1.84 kPa and 18.4 kPa) as fixed factors and leaves as random factor nested within plant type. The effects of plant type, O_2 level, and plant type×O_2 level interaction on A, g_{sC}, C_i, C_i/C_a, Δ_o, C_c, Γ, $R_{d(6m)}$, $\delta^{13}C_{Rd(6m)}$, $R_{d(30m)}$, $\delta^{13}C_{Rd(30m)}$, $R_{d(3h)}$, and $\delta^{13}C_{Rd(3h)}$ were assessed. A PROC MIXED procedure was

Table 1. *Description of the abbreviations, symbol, value (as in Evans and von Caemmerer, 2013), and unit of the environmental parameters and leaf variables used in this study*

Abbreviation	Description
G_{ch}	Growth chamber
GDC	Glycine decarboxylase complex
gdch-KD	Transgenic GDC H-subunit knockdown
L_{ch}	Leaf chamber
LEDR	Light-enhanced dark respiration
NH_3	Ammonia
NH_4^+	Ammonium cation
PDH	Pyruvate dehydrogenase
RuBP	Ribulose 1,5-bisphosphate
TCA	Tricarboxylic acid
2-PG	2-phosphoglycolate
3-PGA	3-phosphoglycerate

Symbol	Environmental parameters/leaf variables	Value and unit
A	Net CO_2 assimilation rate per unit (one side) leaf surface area	µmol CO_2 m^{-2} s^{-1}
a	^{13}C fractionation during CO_2 diffusion (in air) through stomata	4.4‰
b_3	Rubisco ^{13}C fractionation	29.0‰
C_a	CO_2 mole fraction or CO_2 partial pressure set in the leaf chamber	µmol mol^{-1}; Pa
C_c	CO_2 mole fraction or CO_2 partial pressure in the chloroplast	µmol mol^{-1}; Pa
C_i	CO_2 mole fraction or CO_2 partial pressure in the intercellular air space	µmol mol^{-1}; Pa
C_{in}	CO_2 mole fraction entering the leaf chamber	µmol mol^{-1}
C_{out}	CO_2 mole fraction leaving the leaf chamber	µmol mol^{-1}
C_s	CO_2 mole fraction at the leaf surface	µmol mol^{-1}
f	Photorespiratory $^{13}CO_2$ fractionation	‰
g_m	Mesophyll conductance to CO_2 diffusion from the substomatal cavity to the chloroplast stroma	µmol CO_2 m^{-2} s^{-1} Pa^{-1}
g_{sC}	Stomatal conductance to CO_2 diffusion	µmol CO_2 m^{-2} s^{-1} Pa^{-1}
LMA	Leaf dry mass per (one side) unit surface area	g m^{-2}
pCO_2	Partial pressure of CO_2	Pa
pO_2	Partial pressure of O_2	kPa
PPFD	Photosynthetic photon flux density	µmol photons m^{-2} s^{-1}
R_d	Dark respiration rate per unit (one side) leaf surface area	µmol CO_2 m^{-2} s^{-1}
$R_{d(24h)}$	R_d after 24 h dark	µmol CO_2 m^{-2} s^{-1}
$R_{d(30min)}$	R_d after 30 min dark	µmol CO_2 m^{-2} s^{-1}
$R_{d(3h)}$	R_d after 3 h dark	µmol CO_2 m^{-2} s^{-1}
$R_{d(6min)}$	R_d after 6 min dark	µmol CO_2 m^{-2} s^{-1}
R_L	Light mitochondrial non-photorespiratoy respiration rate per unit (one side) leaf surface area	µmol CO_2 m^{-2} s^{-1}
t	Correction factor for ternary effects	‰
t_{air}	Air temperature	°C
t_{leaf}	Leaf temperature	°C
VPD	Vapor pressure deficit	kPa
α	Moles of CO_2 released in the photorespiratory pathway per mole of O_2 reacting with RuBP	mol CO_2 mol^{-1} O_2
Δ_e	^{13}C discrimination associated wtih mitochondrial non-photorespiratory respiration	‰
Δ_f	^{13}C discrimination associated with photorespiration	‰
Δ_{gm}	^{13}C discrimination associated with mesophyll conductance to CO_2 diffusion	‰
Δ_i	^{13}C discrimination due to carboxylation, boundary layer and stomatal CO_2 diffusion	‰
Δ_o	Observed (instantaneous) leaf net discrimination against $^{13}CO_2$ in the light	‰
Γ	CO_2 compensation point	µmol mol^{-1}; Pa
Γ^*	CO_2 compensation point in absence of mitochondrial non-photorespiratory respiration	µmol mol^{-1}; Pa
δ_{in}	$\delta^{13}C$ of CO_2 entering the leaf chamber	‰
δ_{out}	$\delta^{13}C$ of CO_2 leaving the leaf chamber	‰
$^{\delta Rd}G_{ch\_substr}$	Fractional contribution of respiratory substrates from G_{ch} carbon assimilates to $\delta^{13}C$ of dark-evolved CO_2	‰/‰
$^{\delta Rd}L_{ch\_substr}$	Fractional contribution of respiratory substrates from L_{ch} carbon assimilates to $\delta^{13}C$ of dark-evolved CO_2	‰/‰
$\delta^{13}C$	^{13}C composition of CO_2	‰
$\delta^{13}C_{dm}$	^{13}C signature of leaf dry matter	‰
$\delta^{13}C_{Gch}$	^{13}C composition of atmospheric CO_2 in the growth chamber during the photoperiod	‰
$\delta^{13}C_{Lch\_Ph}$	Representative $\delta^{13}C$ of carbon assimilates produced in the L_{ch}	‰
$\delta^{13}C_{Rd}$	$\delta^{13}C$ of CO_2 evolved by leaves in the dark	‰
$\delta^{13}C_{Rd(24h)}$	$\delta^{13}C$ of CO_2 evolved by leaves after 24 h dark	‰
$\delta^{13}C_{Rd(30min)}$	$\delta^{13}C$ of CO_2 evolved by leaves after 30 min dark	‰
$\delta^{13}C_{Rd(3h)}$	$\delta^{13}C$ of CO_2 evolved by leaves after 3 h dark	‰
$\delta^{13}C_{Rd(6min)}$	$\delta^{13}C$ of CO_2 evolved by leaves after 6 min dark	‰

applied as a one-way ANOVA to determine the plant type (fixed factor) effect on the following traits: total N content, malate content, $\Gamma^{\star}$, Δ_o, Δ_i, $\Delta_i-\Delta_o$, Δ_{gm}, Δ_e, Δ_f, $R_{d(24h)}$, $\delta^{13}C_{Rd(24h)}$, LMA, and $\delta^{13}C_{dm}$. A one-sample *t*-test ($P<0.05$) was applied to test the difference of *f* or α modeled for the *gdch*-KD plants compared with a constant *f* or α value assumed in the WT. A two-sample *t*-test ($P<0.05$) was applied to test the difference between *gdch*-KD and WT g_m at a pO_2 of 1.84 kPa, and WT g_m at the two O_2 levels. For each plant type, a three-parameter non-linear model was fit to the R_d and $\delta^{13}C_{Rd}$ responses determined over the 195 min in the dark after leaf photosynthesis at each O_2 experimental level. In particular, the $\delta^{13}C_{Rd}$ values associated with the lower O_2 level had been first edited as described in Supplementary Methods S7, and then used for the analysis. The fitting model $y=\theta_1 e-\theta_2 x+\theta_3$ was employed where *x* are minutes from 0 to 195 by steps of three, and *y* are R_d or $\delta^{13}C_{Rd}$ values; θ_1, θ_2, and θ_3 are the range, slope, and lower asymptote (or floor) parameters, respectively, which were determined using non-linear least squares with the iterative Gauss–Newton algorithm. Specifically, for R_d or $\delta^{13}C_{Rd}$ responses, the range parameter corresponds to the difference between initial and lower asymptote values, and the slope is the exponential rate of change. An extra sum of squares *F*-test was applied to define the significance ($P<0.05$) of the effects of plant type and O_2 level (main effects), and plant type×O_2 level interactions on the three parameters of R_d or $\delta^{13}C_{Rd}$ fitting models.

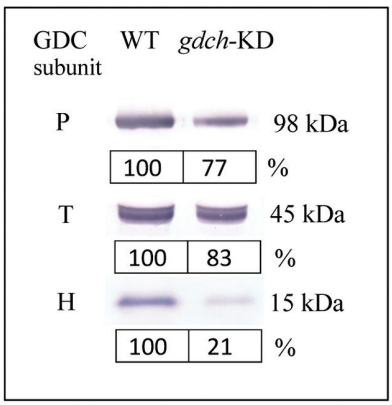

Fig. 1. Immunoblot analysis for GDC P-, T-, and H-subunits in mature leaves of *gdch*-KD compared with WT plants. The protein molecular weight of each subunit (kDa) is shown. Subunit protein abundances for *gdch*-KD plants are mean percentage values of the WT ($n=2$).

Results

Leaf GDC protein and malate content

Leaves of *gdch*-KD plants had 21% (±2 SE) H-protein content compared with the WT, while the P- and T-protein content was 77% (±6 SE) and 83% (±2 SE) of that of the WT, respectively (Fig. 1; $n=2$). Malate content in leaf samples taken immediately after measurements of leaf photosynthesis were 0.49±0.08 mmol m^{-2} and 0.38±0.02 mmol m^{-2} (mean ±SE; $n=5$) in *gdch*-KD and WT plants, respectively ($P=0.29$).

Leaf physiological analysis

Leaf photosynthetic responses

There was no observable difference in growth phenotypes between the *gdch*-KD and WT plants when they were grown under 184.2 Pa pCO_2 (2000 µmol mol^{-1}). However, at approximately current ambient CO_2 and O_2 partial pressures, the net rate of CO_2 assimilation (*A*) was lower in the *gdch*-KD compared with the WT but there was no significant difference in *A* between plant types under low photorespiratory conditions, when pO_2 was reduced to 1.84 kPa (Table 2). There was, however, a significant effect of O_2 level on g_{sC} (negative effect) and C_i/C_a (positive effect) but not a plant type effect (Table 2). There was a significant plant type×O_2 level interaction on Δ_o, which showed higher values for the *gdch*-KD compared with the WT at a pO_2 of 18.4 kPa, but no difference at a pO_2 of 1.84 kPa (Table 2). There was no significant plant type effect on g_m at a pO_2 of 1.84 kPa ($P=0.586$), and no O_2 effect on g_m in the WT ($P=0.701$; Table 2). There was, however, a significant effect of plant type on C_c, which showed comparable values in the *gdch*-KD and WT plants at 1.84 kPa pO_2 and higher values in the *gdch*-KD plants compared with the WT at 18.4 kPa pO_2 (modeled based on equal g_m in both transgenic and WT plants). In addition, O_2 level had a positive effect on C_c (Table 2). The Γ in the *gdch*-KD compared with WT plants was significantly lower under 1.84 kPa pO_2 but higher under 18.4 kPa pO_2 (Table 3). There was no significant difference in

Table 2. *Leaf photosynthetic traits estimated on* gdch-*KD and WT plants under approximately current ambient and below current ambient O_2 levels (*pO_2 *of 18.4 kPa and 1.84 kPa, respectively) at* C_a *of 27.6 Pa.*

Plant-type	pO_2 (kPa)	*A* (µmol CO_2 m^{-2} s^{-1})	g_{sC} (µmol CO_2 m^{-2} s^{-1} Pa^{-1})	C_i (Pa)	C_i/C_a	g_m[a] (µmol CO_2 m^{-2} s^{-1} Pa^{-1})	C_c (Pa)	Δ_o (‰)
gdch-KD	1.84	24.7±1.4	3.47±0.53	18.1±0.8	0.66±0.03	4.56±0.43	12.6±1.4	14.9±0.7
	18.4	6.3±0.3	1.37±0.11	22.1±0.2	0.80±0.01		20.6±0.2	23.7±0.5
WT	1.84	21.6±1.2	2.78±0.43	18.5±0.9	0.67±0.03	3.80±0.76	12.6±0.5	14.3±0.8
	18.4	14.3±0.8	2.45±0.31	20.5±0.5	0.74±0.02	4.07±0.14	17.0±0.6	17.8±0.3
Significance	Plant type	$P=0.050$	$P=0.629$	$P=0.411$	$P=0.411$	–	$P=0.031$	$P=0.003$
	pO_2	$P<0.001$	$P=0.018$	$P=0.003$	$P=0.003$	–	$P=0.000$	$P<0.001$
	Plant type×pO_2	$P=0.002$	$P=0.057$	$P=0.171$	$P=0.171$	–	$P=0.033$	$P=0.003$

Values are the mean±SE ($n=4$). Significance ($P<0.05$) of the effects of plant type, pO_2, and plant type×pO_2 interaction were evaluated by SAS PROC MIXED.

[a] No significant differences were evaluated by a two sample *t*-test (significance for $P<0.05$) between the *gdch*-KD and WT g_m values at a pO_2 of 1.84 kPa ($P=0.586$), and the WT g_m values at the two pO_2 values ($P=0.701$).

leaf N content between plant types, with means of 2.30±0.08 SE g m^{-2} and 2.31±0.14 SE g m^{-2} in *gdch*-KD and WT leaves, respectively (n=4).

Δ_o plotted versus C_i/C_a showed a similar response in the *gdch*-KD and WT plants at 1.84 kPa pO_2 but was significantly greater in the *gdch*-KD compared with WT plants at 18.4 kPa pO_2 (Fig. 2; see Table 2 for statistical analysis). The *gdch*-KD plants had significantly lower Δ_{gm}, Δ_f, and Δ_e compared with the WT under a pO_2 of 18.4 kPa (Fig. 3A). Additionally, the *gdch*-KD plants had a significantly lower f with mean values of 3.4±0.5‰ SE (n=4) compared with 16.2‰ in the WT under approximately current ambient pO_2 (Fig. 3B; P<0.001). A significantly higher α was determined at 18.4 kPa pO_2 in *gdch*-KD plants, with a mean value of 0.59±0.01 SE (n=3), versus 0.5 assumed for the WT (P<0.01). There was a negative linear dependency of f on Γ^* and on α (Supplementary Methods S5; Fig. S1A and B, respectively); however, there was a positive linear dependency of f on g_m and R_L, with a greater sensitivity to g_m (Supplementary Fig. S2A ands B, respectively).

Leaf dark respiration responses

In the *gdch*-KD and WT plants, the R_d showed a hyperbolic decrease over the 3 h in the dark after leaf light exposure under different O_2 levels, with a noticeable rapid decline in the first hour; however, R_d was higher following leaf photosynthesis at a pO_2 of 18.4 kPa compared with 1.84 kPa. (Fig. 4). A significant positive O_2 effect on R_d responses of *gdch*-KD and WT plants was inferred based on significantly higher floor (μmol CO_2 m^{-2} s^{-1}; P<0.0001) and range (μmol CO_2 m^{-2} s^{-1}; P<0.0001) parameters after leaf photosynthesis at pO_2 of 18.4 kPa compared with 1.84 kPa in the non-linear model fit to the R_d responses (Supplementary Tables S3, S4). In particular, based on the spot measurements, a significant positive O_2 effect was determined on $R_{d(6min)}$ (together with a significant plant type effect), $R_{d(30min)}$, and $R_{d(3h)}$ (Table 4). A significant plant type effect on R_d responses was inferred based on a statistically larger range (P=0.023) and less steep rate of exponential change (slope, μmol CO_2 m^{-2} s^{-1} min^{-1}; P<0.0001) for the *gdch*-KD versus WT plants (Supplementary Tables S3, S4). After leaf photosynthesis at a pO_2 of 18.4 kPa, a significant plant type effect on R_d (with higher R_d determined in the *gdch*-KD plants versus the WT; see Fig. 4) was driven by the significantly less steep R_d slope (P<0.001) in *gdch*-KD compared with WT plants. In addition, following leaf photosynthesis at a pO_2 of 18.4 kPa, a change in R_d for ~75% of the R_d range occurred in WT plants within the first 30 min after light–dark transition; in contrast, this fractional variation took ~90 min in the *gdch*-KD plants (Fig. 4). The mean values of R_L inferred from $R_{d(3h)}$ were 0.59±0.03 SE μmol CO_2 m^{-2} s^{-1} for *gdch*-KD and 0.56±0.03 SE μmol CO_2 m^{-2} s^{-1} for WT plants after leaf photosynthesis under a pO_2 of 1.84 kPa (n=4). In contrast, R_L was 0.98±0.12 SE μmol CO_2 m^{-2} s^{-1} for *gdch*-KD and 0.82±0.09 SE μmol CO_2 m^{-2} s^{-1} for WT plants after leaf exposure to a pO_2 of 18.4 kPa (n=4). For the R_L values, a non-significant plant type effect and a significant effect of the O_2 level can be inferred from the significance of $R_{d(3h)}$ (see Table 4). In addition, no significant difference in leaf dry mass per unit surface area (LMA) was determined between *gdch*-KD and WT plants, with values of 43.6±2.7 SE g m^{-2} and 44.5±1.5 SE g m^{-2} (n=4), respectively.

In *gdch*-KD and WT plants, the $\delta^{13}C_{Rd}$ estimated over the 3 h after light–dark transition showed a negative hyperbolic pattern, with most of the $\delta^{13}C_{Rd}$ variation occurring in the first 30 min (Fig. 5A, B). A tight positive correlation between R_d and $\delta^{13}C_{Rd}$ over the 3 h dark period was determined after leaf photosynthesis at a pO_2 of 1.84 kPa for both plant types (r>0.90). After leaf photosynthesis at a pO_2 of 18.4 kPa, a positive correlation between R_d and $\delta^{13}C_{Rd}$ with r=0.75 and r=0.78 was determined for *gdch*-KD and the WT, respectively. Statistical analysis of a non-linear model fit to the $\delta^{13}C_{Rd}$ responses showed a significantly lower $\delta^{13}C_{Rd}$ range after leaf photosynthesis at a pO_2 of 18.4 kPa (‰; P<0.0001) compared with 1.84 kPa pO_2. In contrast, the floor parameter was non-significantly different between the O_2 levels (Supplementary Tables S5, S6). These statistical results indicate a significant effect of the O_2 level during previous leaf light exposure on

Table 3. *CO_2 compensation points (Γ) determined under low photorespiratory (1.84 kPa pO_2) and photorespiratory (18.4 kPa pO_2) conditions on* gdch*-KD and WT plants*

Plant-type	pO_2 (kPa)	Γ (Pa)
gdch-KD	1.84	0.25±0.06
	18.4	5.48±0.04
WT	1.84	0.62±0.12
	18.4	4.54±0.18
Significance	Plant type	P=0.055
	pO_2	P<0.001
	Plant type×pO_2	P=0.001

Values are the mean ±SE (n=3 for *gdch*-KD at a pO_2 of 18.4 kPa; n=4 otherwise). Significance (P<0.05) for the effects of plant type, pO_2, and plant type×pO_2 interaction was evaluated by SAS PROC MIXED.

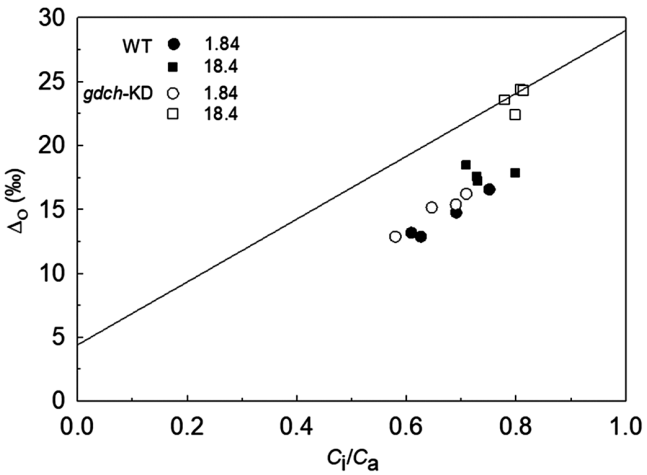

Fig. 2. Leaf $^{13}CO_2$ net discrimination in the light (Δ_o) versus C_i/C_a under a pO_2 of 1.84 kPa and 18.4 kPa for individual *gdch*-KD and WT plants. The line represents the leaf $^{13}CO_2$ net discrimination modeled in relation to C_i/C_a as $\Delta^{13}C_{mod}=a+(b_3-a)\times C_i/C_a$ (Farquhar *et al.*, 1982) where a=4.4‰ and b_3=29.0‰. $\Delta^{13}C_{mod}$ is a proxy of Δ_i as described by Evans and von Caemmerer (2013). Open symbols are for *gdch*-KD and filled symbols for WT plants. Circles are for a pO_2 of 1.84 kPa and squares for a pO_2 of 18.4 kPa.

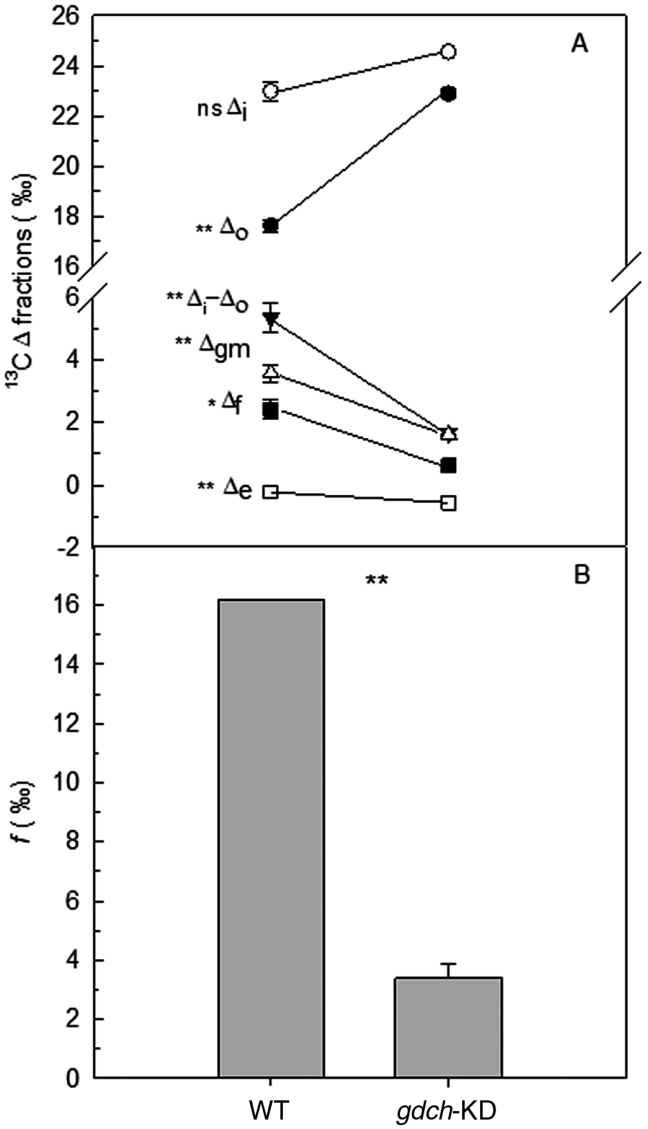

Fig. 3. Leaf $^{13}CO_2$ net discrimination and discrimination fractions in the light, and $^{13}CO_2$ photorespiratory fractionation for *gdch*-KD versus WT plants determined based on Evans and von Caemmerer (2013). (A) Observed leaf net $^{13}CO_2$ discrimination in the light (Δ_o), and modeled ^{13}C discrimination fractions for *gdch*-KD (n=3) and the WT (n=4) at an atmospheric pO_2 of 18.4 kPa. Δ_i is the additive $^{13}CO_2$ discrimination during CO_2 diffusion from atmosphere to intercellular air space and due to carboxylation; Δ_i–Δ_o is comprised of three terms: Δ_{gm}, which is the $^{13}CO_2$ fractionation fraction during CO_2 diffusion in the liquid phase to chloroplast stroma, and Δ_e and Δ_f, which are the ^{13}C fractionation fractions associated with light mitochondrial non-photorespiratory respiration and photorespiration, respectively. Δ_f was calculated as $\Delta_f=\Delta_i-\Delta_o-\Delta_{gm}-\Delta_e$. Values are mean ±SE. (B) $^{13}CO_2$ fractionation for photorespiration (f) in *gdch*-KD plants calculated at an atmospheric pO_2 of 18.4 kPa from $\Delta_f = \frac{1+t}{1-t}\left(f\frac{\Gamma^*}{C_a}\right)$ versus f of 16.2‰ in the WT. Values for *gdch*-KD plants are the mean ±SE (n=3). Significance (P<0.05) of the effect of plant type on the variables in (A) was evaluated by SAS PROC MIXED as a one-way ANOVA; * for 0.01<P<0.05; ** for P<0.01. Significance in (B) was evaluated by one-sample t-test (P<0.05). ** for P<0.01.

the $\delta^{13}C_{Rd}$ values of both plant types over 3 h in the dark (with lower $\delta^{13}C_{Rd}$ at a pO_2 of 18.4 kPa, and higher $\delta^{13}C_{Rd}$ at a pO_2 of 1.84 kPa). The spot $\delta^{13}C_{Rd}$ measurements also showed significantly lower $\delta^{13}C_{Rd(6min)}$ and $\delta^{13}C_{Rd(30min)}$ after leaf photosynthesis at a pO_2 of 18.4 kPa compared with 1.84 kPa (Table 4). There was no significant plant type effect on the $\delta^{13}C_{Rd}$ over the 3 h in the dark (Table 4; Supplementary Table S6) and there was no difference for $\delta^{13}C_{dm}$ between *gdch*-KD and the WT (Supplementary Table S1).

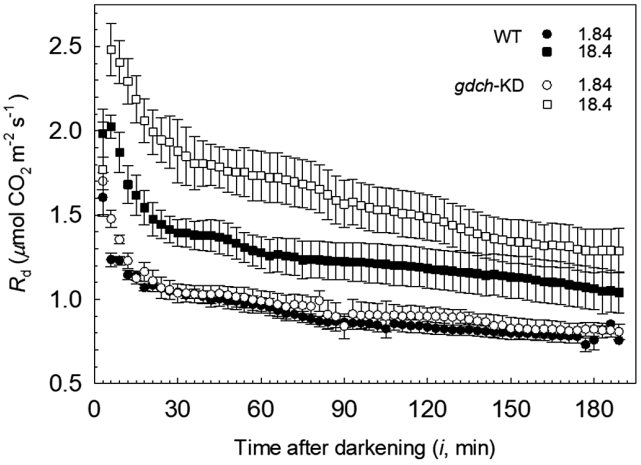

Fig. 4. Dynamics of leaf dark respiration rate (R_d) determined during ~3 h in the dark on *gdch*-KD (open symbols) and WT (filled symbols) plants after leaf photosynthesis under a pO_2 of 1.84 kPa (circles) or 18.4 kPa (squares). Symbols correspond to the mean ±SE (n=4) determined every 3 min.

Over the 3 h after the light–dark transition, the fractional contribution of L_{ch} assimilates to $\delta^{13}C_{Rd}$ ($\delta^{Rd}L_{ch\_substr}$, ‰/‰) showed a decreasing hyperbolic pattern for both *gdch*-KD and WT plants (Fig. 6), with no significant differences between plant types and O_2 levels.

Discussion

Altered photorespiratory metabolism and leaf photosynthetic traits

Based on leaf protein analysis, *gdch*-KD plants had ~21, 77, and 83% of GDC H-, P-, and T-protein abundance, respectively, compared with the WT. Previous studies reported how GDC activity is linearly correlated with H-protein accumulation (Wingler *et al.*, 1997; Lin *et al.*, 2016). Additionally, in agreement with Lin *et al.* (2016), the *gdch*-KD plants in the current study showed an expected photorespiratory-deficient phenotype. Under photorespiratory conditions, a disruption of the photorespiratory pathway negatively affects the rate of net CO_2 assimilation (A) due to accumulation of metabolites that inhibit the Calvin–Benson cycle and restrict RuBP regeneration (Wingler *et al.*, 2000). Specifically, leaf glycine level is a sensitive indicator of altered photorespiratory carbon flow (Blackwell *et al.*, 1988; Timm *et al.*, 2012). For example, *gdch*-KD mutants of Arabidopsis, barley, and rice had substantial increases in leaf contents of glycine under ambient pO_2 (Bauwe and Kolukisaoglu, 2003; Lin *et al.*, 2016). This accumulation of glycine and its precursors (P-glycolate, glycolate, and glyoxylate) in the *gdch*-KD plants has been suggested to alter photorespiratory carbon metabolism (Peterhansel *et al.*, 2010, 2013*a*). These changes have important implications for understanding and modeling leaf carbon metabolism, because they

Table 4. *Leaf dark respiration rates (R_d) at 30 °C and $^{13}CO_2$ composition of dark-evolved CO_2 ($\delta^{13}C_{Rd}$) determined on* gdch-*KD versus the WT after 6 min [$R_{d(6min)}$ and $\delta^{13}C_{Rd(6min)}$; n=4], 30 min [$R_{d(30min)}$ and $\delta^{13}C_{Rd(30min)}$; n=4], 3 h [$R_{d(3h)}$ and $\delta^{13}C_{Rd(3h)}$; n=4], and 24 h [$R_{d(24h)}$ and $\delta^{13}C_{Rd(24h)}$; n=3] in the dark following leaf exposure to light under approximately current ambient and below current ambient O_2 levels (pO_2 of 18.4 kPa and 1.84 kPa, respectively)*

Plant-type	pO_2 (kPa)	$R_{d(6min)}$ (μmol CO_2 m^{-2} s^{-1})	$\delta^{13}C_{Rd(6min)}$ (‰)	$R_{d(30min)}$ (μmol CO_2 m^{-2} s^{-1})	$\delta^{13}C_{Rd(30min)}$ (‰)	$R_{d(3h)}$ (μmol CO_2 m^{-2} s^{-1})	$\delta^{13}C_{Rd(3h)}$ (‰)	$R_{d(24h)}$ (μmol CO_2 m^{-2} s^{-1})	$\delta^{13}C_{Rd(24h)}$ (‰)
gdch-KD	1.84	1.48±0.05	−39.2±0.9*	1.04±0.06	−47.3±1.6*	0.81±0.04	−56.0±0.7*	0.79±0.02	−58.0±0.5*
WT	1.84	1.23±0.04	−40.6±1.2*	1.04±0.01	−47.2±1.7*	0.77±0.04	−54.1±0.7*	0.69±0.02	−58.6±1.0*
Significance								*P*=0.045	*P*=0.705
gdch-KD	18.4	2.59±0.29	−45.6±1.7	1.98±0.20	−54.1±0.9	1.34±0.17	−55.6±1.2	0.69±0.06	−58.1±0.1
WT	18.4	2.13±0.07	−43.2±0.9	1.47±0.08	−50.4±2.8	1.12±0.13	−52.5±1.8	0.74±0.08	−58.6±0.6
Significance	Plant type	*P*=0.042	*P*=0.723	*P*=0.110	*P*=0.349	*P*=0.215	*P*=0.132	*P*=0.596	*P*=0.410
	pO_2	*P*=0.0001	*P*=0.032	*P*=0.0009	*P*=0.035	*P*=0.004	*P*=0.429	–	–
	Plant type×pO_2	*P*=0.407	*P*=0.238	*P*=0.069	*P*=0.375	*P*=0.326	*P*=0.753	–	

Values are the mean ±SE; the asterisks indicate means from $\delta^{13}C_{Rd}$ values edited according to Supplementary Method S7. Significance (P<0.05) of the effects of plant type, pO_2, and plant type×pO_2 interaction was evaluated by SAS PROC MIXED. The effect of plant type on $R_{d(24h)}$ and $\delta^{13}C_{Rd(24h)}$ was evaluated at a pO_2 of 1.84 kPa or 18.4 kPa by one-way ANOVA (significance for P<0.05).

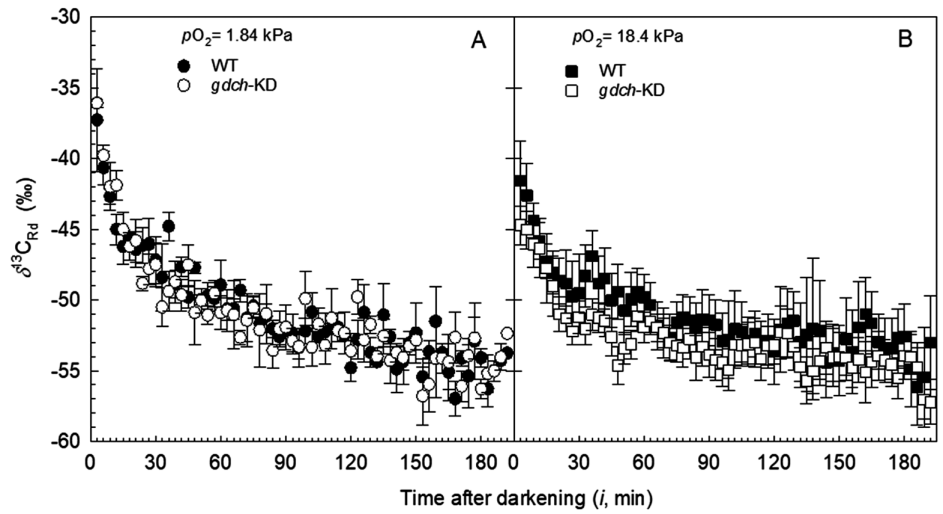

Fig. 5. $^{13}CO_2$ composition associated with R_d ($\delta^{13}C_{Rd}$) determined during ~3 h in the dark in *gdch*-KD (open symbols) and WT (filled symbols) plants. (A) $\delta^{13}C_{Rd}$ after leaf photosynthesis under a pO_2 of 1.84 kPa edited (see Supplementary Methods S7) to remove the effect of a lower atmospheric $\delta^{13}CO_2$ compared with (B) while growing the plants. (B) Distributions of $\delta^{13}C_{Rd}$ after leaf photosynthesis under a pO_2 of 18.4 kPa. Symbols correspond to the mean ±SE (n=4) determined every 3 min.

may influence the stoichiometry of CO_2 released per oxygenation reaction (α) and the CO_2 compensation point (Γ) (see Cousins *et al.*, 2008, 2011; Walker and Cousins, 2013).

In the present study, the *gdch*-KD plants had greater Γ compared with the WT under 18.4 kPa pO_2, as previously reported by Lin *et al.* (2016). This may be partially due to enhanced R_L, which Igamberdiev *et al.* (2004) and Bykova *et al.* (2005) reported was needed to compensate for the lack of photorespiratory regulation of redox and energy balance (Igamberdiev *et al.*, 2001). The increase in Γ in the *gdch*-KD plants could also be associated with a higher α leading to an increasing Γ^* compared with the WT. It has been previously suggested that α increased in Arabidopsis mutants lacking peroxysomal hydroxypuruvate reductase (Cousins *et al.*, 2008) and the peroxysomal malate dehydrogenase (Cousins *et al.*, 2011). However, these previous publications did not determine whether these disruptions to photorespiration influenced leaf CO_2 isotope exchange.

Leaf net ^{13}C discrimination in the light and photorespiratory ^{13}C fractionation

Under leaf photorespiratory conditions, the change in leaf net discrimination against $^{13}CO_2$ (Δ_o) in the *gdch*-KD plants

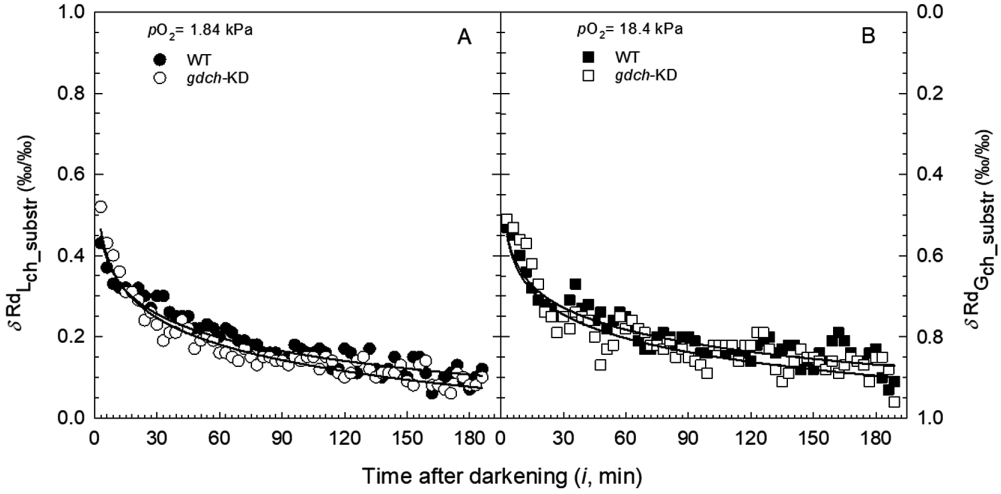

Fig. 6. Distributions over ~3 h in the dark of the fractional contributions (total contribution equal to 1.0) to $\delta^{13}C_{Rd}$ of recent L_{ch} carbon assimilates ($\delta^{Rd}L_{ch\_substr}$, ‰/‰) and G_{ch} assimilates ($\delta^{Rd}G_{ch\_substr}$, ‰/‰) for *gdch*-KD (open symbols) and WT (filled symbols) after leaf light exposure at a pO_2 of (A) 1.84 kPa and (B) 18.4 kPa. The first values are at 3 min after light–dark transition. Symbols correspond to the mean determined every 3 min (n=4). Continuous lines represent logarithmic trend lines (R^2 >0.90) for *gdch*-KD (lower) and the WT (higher), respectively.

compared with WT plants was caused by a higher C_i/C_a, lower Δ_{gm}, greater Δ_e, and lower Δ_f (Fig. 3A). However, the lower Δ_{gm} in the *gdch*-KD plants with respect to the WT was due to a reduction in A, since WT g_m was applied to both plant types (see Δ_{gm} equation in Evans and von Caemmerer, 2013). In addition, a difference in Δ_e between *gdch*-KD and WT plants was related to proportional changes in $R_L/(A+R_L)$ and $(C_i-\Gamma^*)$ (see Δ_e equation in Evans and von Caemmerer, 2013).

The term Δ_f is dependent on $\frac{\Gamma^*}{C_a}$, but, despite the higher Γ^* in the *gdch*-KD relative to WT plants, it was lower in the transgenic plants caused by the lower f. In WT plants, f is primarily attributed to the ^{13}C discrimination associated with the decarboxylation of glycine catalyzed by GDC (Tcherkez *et al.*, 2004; Tcherkez, 2006). While Rooney (1988) determined an *in vitro* f of 7–8‰ for *Glycine max* (soybean), Igamberdiev *et al.* (2001, 2004) reported f for several species between 9.8 and 13.7‰, and Ghashghaie *et al.* (2003) reported an f of >9–11‰ for *Senecio* species. Additionally, Evans and von Caemmerer (2013) determined an *in vivo* f of 16.2‰ in *Nicotiana tabacum*. Based on Farquhar *et al.* (1982), and according to O'Leary (1988) and Tcherkez (2006),

$$f = (\delta^{13}C_{glycine} - \delta^{13}C_{photorespired\_CO2}) / (1 + \delta^{13}C_{photorespired\_CO2}/1000) \quad (3)$$

where glycine is assumed to have the same ^{13}C signature of recently fixed carbon. Therefore, an increase in $\delta^{13}C$ of the released CO_2 during photorespiration corresponds to a linear decrease in f. There is also a negative linear dependency of f on Γ^* and α, as shown in Supplementary Methods S5; Fig. S1A, B.

In C_3 plants, most of the CO_2 released by photorespiration tends to be through GDC (Badger, 1985; Bauwe *et al.*, 2010). However, previous reports have suggested that alternative reactions can release CO_2 when the flux of glycolate into the photorespiratory cycle exceeds its metabolic capacity, or when the traditional photorespiratory pathway has been genetically disrupted (Cousins *et al.*, 2008, 2011; Timm *et al.*, 2008; Peterhansel *et al.*, 2013*a*). The GDC multienzyme system requires all subunits to function (Douce *et al.*, 2001); in the present study, since a low level of the H-subunit was determined in *gdch*-KD plants, some residual activity for GDC is expected in the transgenic plants. A change in ^{13}C fractionation associated with the knockdown of GDC activity is therefore unlikely because the products of the glycine decarboxylation reaction (NH_4^+, NADH, and methylene-tetrahydrofolate) can be readily processed by downstream reactions in the glycolate pathway (Bauwe *et al.*, 2010; Maurino and Peterhansel, 2010). Thus, the higher α and lower f in the *gdch*-KD compared with the WT suggest an increased flow of photorespiratory carbon through alternative decarboxylation reactions, independent of the GDC, and a buildup of photorespiratory metabolites.

Leaf dark respiration and ^{13}C isotopic composition of dark-evolved CO_2

Leaves of C_3 plants in the first 30 min after light–dark transition largely respire metabolites (carbohydrates and organic acids) recently produced in the light (Cornic, 1973; Rademacher *et al.*, 2002; Barbour *et al.*, 2007; Werner *et al.*, 2009; Werner and Gessler, 2011; Lehmann *et al.*, 2015, 2016) and show high rates of CO_2 evolution (named as LEDR, light-enhanced dark respiration; Atkin *et al.*, 1998). While the activity of pyruvate dehydrogenase (PDH) and metabolism in the tricarboxylic acid (TCA) cycle are the major mitochondrial decarboxylations in the dark, they are partially inhibited in the light (Ghashghaie *et al.*, 2003; Tcherkez *et al.*, 2005, 2008; Barbour *et al.*, 2007). It has been suggested that LEDR mostly depends on a buildup of malate and fumarate in the light, which are then rapidly decarboxylated after the light–dark transition (Atkin *et al.*, 1998; Barbour *et al.*, 2007; Tcherkez *et al.*, 2012). However, there is evidence for species-specific differences (Lehmann *et al.* 2016; Gessler *et al.*, 2017). Overall, R_d in the *gdch*-KD and WT plants showed an expected negative hyperbolic pattern during 3 h in the dark following leaf photosynthesis. The results of the

present study indicate that leaf photosynthesis under photorespiring conditions, before the light–dark transition, led to an additional buildup of TCA cycle substrates in the *gdch*-KD plants compared with the WT. In fact, the *gdch*-KD plants had a significantly higher R_d over 3 h dark following leaf photosynthesis under the approximately current ambient O_2 level (with leaf blades having no significantly different LMA), compared with the WT; this suggests a greater accumulation of metabolites in the light, in particular photorespiratory intermediates, as respiratory substrates to feed R_d. More precisely, a restricted photorespiratory pathway in the light may lead to an accumulation of 2-carbon metabolites in the *gdch*-KD plants.

The increase in LEDR has been reported to come from the decarboxylation of ^{13}C heavier metabolites, primarily malate, and the decline in LEDR rates and $\delta^{13}C_{Rd}$ over time due to a decrease in malate availability (Barbour *et al.* 2007; Gessler *et al.*, 2009). In the *gdch*-KD plants, the cumulative leaf respired CO_2 over 30 min after leaf photosynthesis at a pO_2 of 18.4 kPa was 4.1 mmol CO_2 m^{-2} higher with respect to the WT; theoretically, if this enhancement of R_d in the *gdch*-KD plants was due to malate alone this would require ~1 mmol malate m^{-2}. The non-significant differences in the leaf malate content determined during the light period between *gdch*-KD and the WT suggest that metabolites other than malate, such as photorespiratory intermediates, may have contributed to the greater LEDR rates in the *gdch*-KD plants compared with the WT. A substantial part of the malate in leaves is also stored in vacuoles, as observed in C_4 plants (Hatch, 1979; Arrivault *et al.* 2017), and not readily available for LEDR.

In the *gdch*-KD and WT plants presented here, the $\delta^{13}C_{Rd}$ decreased during the 3 h dark period, tracking the decline in R_d (Fig. 5A, B). Over the 3 h of darkness, there was an increase in the contribution to $\delta^{13}C_{Rd}$ from respiratory substrates generated during plant growth ($^{\delta Rd}G_{ch\_substr}$, ‰/‰) for both plant types and O_2 experimental conditions. Regardless of plant type or O_2 treatment, the $^{\delta Rd}L_{ch\_substr}$ went from ~50% after 6 min from the light–dark transition to ~30% after 30 min in the dark, while after 3 h in the dark it represented only ~10% [see Fig. 6; data of $\delta^{13}C_{Rd(3h)}$ approaching $\delta^{13}C_{Rd(24h)}$ are shown in Table 4]. Tcherkez *et al.* (2010) estimated on sunflower (*Helianthus annuus*) that recent assimilates provide 40–60% of the substrates for R_d (via a pool with a half-life of several hours) both in the light and in the dark. A similar contribution of recent assimilates to R_d was determined by Nogués *et al.* (2004) on French bean (*Phaseolus vulgaris*) leaves during ~2 h in the dark following illumination, which indicates that leaf respiration was fed by a mixture of recent and older substrates.

The tendency for a lower leaf $\delta^{13}C_{Rd}$ in *gdch*-KD plants compared with the WT following leaf light exposure under photorespiratory conditions may partially depend on the higher Δ_o in the *gdch*-KD plants during leaf photosynthesis in the L_{ch} at approximately current ambient pO_2. A greater Δ_o would cause (recent) carbon assimilates synthetized in the L_{ch} (Supplementary data Table S1) to produce more depleted respiratory substrates and a lower $\delta^{13}C_{Rd}$ in the *gdch*-KD compared with the WT. It is also possible that higher Δ_o in the *gdch*-KD compared with WT plants during growth under enriched atmospheric pCO_2 and current ambient pO_2 may have produced G_{ch} assimilates feeding R_d over 3 h after the light–dark transition with slightly lower $\delta^{13}C$ compared with the WT.

The ^{13}C fractionation during leaf dark respiration can change depending on species and environmental conditions (Ghashghaie *et al.*, 2003; Priault *et al.*, 2009; Werner *et al.*, 2009; Lehmann *et al.*, 2016). In addition, $\delta^{13}C_{Rd}$ is influenced by the isotopic signatures of respiratory substrates, from diverse non-homogeneous isotope distributions in the substrates (positional effects) and the different relative activities of decarboxylation pathways. However, decreasing $\delta^{13}C_{Rd}$ over time is mainly dependent on the origin of respiratory substrates, where CO_2 released from pyruvate decarboxylation is ^{13}C enriched (compared with total organic matter) but relatively ^{13}C depleted from acetyl-CoA metabolism through the TCA cycle (Tcherkez *et al.*, 2003). Under continuous darkness and constant t_{air}, it has been shown that $\delta^{13}C_{Rd}$ decreases due to a switch in respiratory substrates from carbohydrates to more ^{13}C-depleted substrates such as lipids or proteins (Ghashghaie *et al.*, 2003; Tcherkez *et al.*, 2003).

The similar $\delta^{13}C_{Rd(24h)}$ in *gdch*-KD versus WT plants implies that the long-term substrates for the TCA cycle produced in the G_{ch} were ^{13}C isotopically similar. This is further supported by similar leaf $\delta^{13}C_{dm}$ between the *gdch*-KD and WT plants. Interestingly, $\delta^{13}C_{Rd(24h)}$ was more depleted than $\delta^{13}C_{dm}$, in agreement with Tcherkez *et al.* (2003) who had found that CO_2 evolved in the dark by French bean leaves in a condition of carbohydrate starvation had a lower $\delta^{13}C$ than total leaf organic matter. This denotes potential changes in dark respiration substrates, such as carbohydrate oxidation producing ^{13}C-enriched CO_2 and β-oxidation of fatty acids producing ^{13}C-depleted CO_2 when compared with total organic matter.

Conclusions

Under photorespiratory conditions, the *gdch*-KD plants had altered ^{13}C discrimination fractions in the light, with a lower Δ_f caused by a reduced *f*. This change in Δ_f and the lower Δ_{gm} lead to a higher Δ_o in the *gdch*-KD plants in comparison with the WT. The lower *f* in the *gdch*-KD plants was attributed to a greater α compared with the WT, suggesting the occurrence of alternative photorespiratory reactions in the GDC-impaired plants. In addition, the enhanced R_d in the *gdch*-KD compared with WT plants after photorespiratory leaf photosynthesis indicated that the photorespiratory disruption led to an additional buildup of metabolites in the light that were decarboxylated by the TCA cycle in the dark. The tendency for a more depleted $\delta^{13}C_{Rd}$ in the *gdch*-KD plants compared with the WT after photorespiratory leaf photosynthesis was mainly ascribed to a higher Δ_o before the light–dark transition and differences in the $\delta^{13}C$ of the substrates feeding R_d. These results indicate that an alteration in photorespiratory carbon metabolism can have a significant effect on leaf CO_2 exchange and $^{13}CO_2$ discrimination, both in the light and in the dark.

Supplementary data

Supplementary data are available at *JXB* online.

Methods S1. Estimate of the $^{13}CO_2$ composition of the growth chamber atmosphere during the light period.

Methods S2. Additional technical information on the system setup to measure online leaf atmosphere CO_2, H_2O, and $^{13}CO_2$ exchange.

Methods S3. Estimate of the ^{13}C signature and total N content in the leaf biomass.

Methods S4. Estimate of the CO_2 compensation point in the absence of mitochondrial non-photorespiratory respiration.

Methods S5. Estimate of α, and evaluation of the sensitivity of f to Γ^* and α (shown in Fig. S1).

Methods S6. Estimate of the fractional contribution of respiratory substrates from leaf chamber and growth chamber carbon assimilates to the ^{13}C composition of dark-evolved CO_2.

Methods S7. Editing of the ^{13}C composition of dark-evolved CO_2 for plants grown at an atmospheric ^{13}C composition of −41.6‰.

Fig. S1 Sensitivity of the f parameter to Γ^* and α.

Fig. S2. Sensitivity of the f parameter to g_m, R_L, and e'.

Table S1. Data used to calculate the fractional contributions of leaf chamber and growth chamber carbon assimilates to ^{13}C composition of leaf dark-evolved CO_2.

Table S2. Values of ^{18}O-based g_m.

Table S3. Statistics for the model used to fit leaf dark respiration rates.

Table S4. Significance for the model used to fit leaf dark respiration rates.

Table S5. Statistics for the model used to fit the ^{13}C composition of leaf dark respiration rates.

Table S6. Significance for the model used to fit ^{13}C composition of leaf dark respiration rates.

Acknowledgements

Research was funded by a C_4 Rice Project grant from The Bill and Melinda Gates Foundation to IRRI (2012–2015) and to the University of Oxford (2015–2019); by the National Science Foundation, grant MCB-1146928; by the National Science Foundation, grant MRI-0923562; and by the Russian Science Foundation, grant 16-16-00089. We thank Charles A. Cody for plant growth management, Dr Raymond W. Lee for ^{13}C analysis on leaf biomass, and Dr Todd Coffey and Dr Marc A. Evans for statistical advice.

Author contributions

SK, SC, H-CL, RAC, WPQ, and JMH generated the transgenic plant material; SvC, RG, RTF, GEE, and ABC planned and designed the experiments; RG performed leaf gas and isotope exchange measurements and analysis; NK performed the biochemical analysis; RG, SvC, RTF, GEE, and ABC interpreted the data; and RG, ABC, and GEE developed the manuscript.

References

Anderson LE. 1971. Chloroplast and cytoplasmic enzymes. II. Pea leaf triose phosphate isomerases. Biochimica et Biophysica Acta **235,** 237–244.

Arrivault S, Obata T, Szecówka M, Mengin V, Guenther M, Hoehne M, Fernie AR, Stitt M. 2017. Metabolite pools and carbon flow during C_4 photosynthesis in maize: $^{13}CO_2$ labeling kinetics and cell type fractionation. Journal of Experimental Botany **68,** 283–298.

Atkin OK, Evans JR, Siebke K. 1998. Relationship between the inhibition of leaf respiration by light and enhancement of leaf dark respiration following light treatment. Functional Plant Biology **25,** 437–443.

Badger MR. 1985. Photosynthetic oxygen exchange. Annual Review of Plant Physiology **36,** 27–53.

Barbour MM, McDowell NG, Tcherkez G, Bickford CP, Hanson DT. 2007. A new measurement technique reveals rapid post-illumination changes in the carbon isotope composition of leaf-respired CO_2. Plant, Cell & Environment **30,** 469–482.

Bauwe H. 2018. Photorespiration—damage repair pathway of the Calvin–Benson cycle. In: Logan DC, ed, Annual Plant Reviews 50. Hoboken, NJ: Wiley-Blackwell, 293–342.

Bauwe H, Hagemann M, Fernie AR. 2010. Photorespiration: players, partners and origin. Trends in Plant Science **15,** 330–336.

Bauwe H, Kolukisaoglu U. 2003. Genetic manipulation of glycine decarboxylation. Journal of Experimental Botany **54,** 1523–1535.

Bernacchi CJ, Singsaas EL, Pimentel C, Portis Jr AR, Long SP. 2001. Improved temperature response functions for models of Rubisco-limited photosynthesis. Plant, Cell & Environment **24,** 253–259.

Betti M, Bauwe H, Busch FA, *et al*. 2016. Manipulating photorespiration to increase plant productivity: recent advances and perspectives for crop improvement. Journal of Experimental Botany **67,** 2977–2988.

Blackwell RD, Murray AJ, Lea PJ, Kendall AC, Hall NP, Turner JC, Wallsgrove RM. 1988. The value of mutants unable to carry out photorespiration. Photosynthesis Research **16,** 155–176.

Bowling DR, Sargent SD, Tanner BD, Ehleringer JR. 2003. Tunable diode laser absorption spectroscopy for stable isotope studies of ecosystem–atmosphere CO_2 exchange. Agricultural and Forest Meteorology **118,** 1–19.

Bykova NV, Keerberg O, Pärnik T, Bauwe H, Gardeström P. 2005. Interaction between photorespiration and respiration in transgenic potato plants with antisense reduction in glycine decarboxylase. Planta **222,** 130–140.

Cornic G. 1973. Etude de l'inhibition de la respiration par la lumière chez la moutarde blanche *Sinapis alba* L. Physiologie Végétale **11,** 663–679.

Cousins AB, Pracharoenwattana I, Zhou W, Smith SM, Badger MR. 2008. Peroxisomal malate dehydrogenase is not essential for photorespiration in *Arabidopsis* but its absence causes an increase in the stoichiometry of photorespiratory CO_2 release. Plant Physiology **148,** 786–795.

Cousins AB, Walker BJ, Pracharoenwattana I, Smith SM, Badger MR. 2011. Peroxisomal hydroxypyruvate reductase is not essential for photorespiration in *Arabidopsis* but its absence causes an increase in the stoichiometry of photorespiratory CO_2 release. Photosynthesis Research **108,** 91–100.

Douce R, Bourguignon J, Neuburger M, Rébeillé F. 2001. The glycine decarboxylase system: a fascinating complex. Trends in Plant Science **6,** 167–176.

Edwards GE, Ku MSB, Hatch MD. 1982. Photosynthesis in *Panicum milioides*, a species with reduced photorespiration. Plant & Cell Physiology **23,** 1185–1195.

Evans JR, Sharkey TD, Berry JA, Farquhar GD. 1986. Carbon isotope discrimination measured concurrently with gas exchange to investigate CO_2 diffusion in leaves of higher plants. Functional Plant Biology **13,** 281–292.

Evans JR, von Caemmerer S. 2013. Temperature response of carbon isotope discrimination and mesophyll conductance in tobacco. Plant, Cell & Environment **36,** 745–756.

Ewald R, Kolukisaoglu U, Bauwe U, Mikkat S, Bauwe H. 2007. Mitochondrial protein lipoylation does not exclusively depend on the mtKAS pathway of de novo fatty acid synthesis in *Arabidopsis*. Plant Physiology **145,** 41–48.

Farquhar GD, O'Leary M, Berry JA. 1982. On the relationship between carbon isotope discrimination and the intercellular carbon dioxide concentration in leaves. Functional Plant Biology **9,** 121–137.

Flexas J, Ribas-Carbó M, Diaz-Espejo A, Galmés J, Medrano H. 2008. Mesophyll conductance to CO_2: current knowledge and future prospects. Plant, Cell & Environment **31,** 602–621.

Gessler A, Roy J, Kayler Z, *et al*. 2017. Night and day—circadian regulation of night-time dark respiration and light-enhanced dark respiration in plant leaves and canopies. Environonmental Experimental Botany **137,** 14–25.

Gessler A, Tcherkez G, Karyanto O, Keitel C, Ferrio JP, Ghashghaie J, Kreuzwieser J, Farquhar GD. 2009. On the metabolic origin of the carbon isotope composition of CO_2 evolved from darkened light-acclimated leaves in *Ricinus communis*. New Phytologist **181,** 374–386.

Ghashghaie J, Badeck F-W, Lanigan G, Nogués S, Tcherkez G, Deléens E, Cornic G, Griffiths H. 2003. Carbon isotope fractionation during dark respiration and photorespiration in C_3 plants. Phytochemistry Reviews **2,** 145–161.

Gillon JS, Griffiths H. 1997. The influence of (photo) respiration on carbon isotope discrimination in plants. Plant, Cell & Environment **20,** 1217–1230.

Giuliani R, Koteyeva N, Voznesenskaya E, Evans MA, Cousins AB, Edwards GE. 2013. Coordination of leaf photosynthesis, transpiration, and structural traits in rice and wild relatives (genus *Oryza*). Plant Physiology **162,** 1632–1651.

Hatch MD. 1979. Mechanism of C_4 photosynthesis in *Chloris gayana*: pool sizes and kinetics of $^{14}CO_2$ incorporation into 4-carbon and 3-carbon intermediates. Archives of Biochemistry and Biophysics **194,** 117–127.

Igamberdiev AU, Bykova NV, Lea PJ, Gardeström P. 2001. The role of photorespiration in redox and energy balance of photosynthetic plant cells: a study with a barley mutant deficient in glycine decarboxylase. Physiologia Plantarum **111,** 427–438.

Igamberdiev AU, Mikkelsen T, Ambus P, Bauwe H, Lea PJ, Gardeström P. 2004. Photorespiration contributes to stomatal regulation and carbon isotope fractionation: a study with barley, potato and *Arabidopsis* plants deficient in glycine decarboxylase. Photosynthesis Research **81,** 139–152.

Jordan DB, Ogren WL. 1984. The CO_2/O_2 specificity of ribulose 1,5-bisphosphate carboxylase/oxygenase: dependence on ribulosebisphosphate concentration, pH and temperature. Planta **161,** 308–313.

Kebeish R, Niessen M, Thiruveedhi K, Bari R, Hirsch HJ, Rosenkranz R, Stäbler N, Schönfeld B, Kreuzaler F, Peterhänsel C. 2007. Chloroplastic photorespiratory bypass increases photosynthesis and biomass production in *Arabidopsis thaliana*. Nature Biotechnology **25,** 593–599.

Kelly GJ, Latzko E. 1976. Inhibition of spinach-leaf phosphofructokinase by 2-phosphoglycollate. FEBS Letters **68,** 55–58.

Kolbe AR, Cousins AB. 2018. Mesophyll conductance in *Zea mays* responds transiently to CO_2 availability: implications for transpiration efficiency in C_4 crops. New Phytologist **217,** 1463–1474.

Koteyeva NK, Voznesenskaya EV, Edwards GE. 2015. An assessment of the capacity for phosphoenolpyruvate carboxykinase to contribute to C_4 photosynthesis. Plant Science **235,** 70–80.

Lanigan GJ, Betson N, Griffiths H, Seibt U. 2008. Carbon isotope fractionation during photorespiration and carboxylation in *Senecio*. Plant Physiology **148,** 2013–2020.

Lehmann MM, Rinne KT, Blessing C, Siegwolf RT, Buchmann N, Werner RA. 2015. Malate as a key carbon source of leaf dark-respired CO_2 across different environmental conditions in potato plants. Journal of Experimental Botany **66,** 5769–5781.

Lehmann MM, Wegener F, Barthel M, Maurino VG, Siegwolf RT, Buchmann N, Werner C, Werner RA. 2016. Metabolic fate of the carboxyl groups of malate and pyruvate and their influence on $\delta^{13}C$ of leaf-respired CO_2 during light enhanced dark respiration. Frontiers in Plant Science **7,** 739.

Lin H, Karki S, Coe RA, *et al*. 2016. Targeted knockdown of *GDCH* in rice leads to a photorespiratory-deficient phenotype useful as a building block for C_4 rice. Plant & Cell Physiology **57,** 919–932.

Maurino VG, Peterhansel C. 2010. Photorespiration: current status and approaches for metabolic engineering. Current Opinion in Plant Biology **13,** 249–256.

Niessen M, Thiruveedhi K, Rosenkranz R, Kebeish R, Hirsch HJ, Kreuzaler F, Peterhänsel C. 2007. Mitochondrial glycolate oxidation contributes to photorespiration in higher plants. Journal of Experimental Botany **58,** 2709–2715.

Nogués S, Tcherkez G, Cornic G, Ghashghaie J. 2004. Respiratory carbon metabolism following illumination in intact French bean leaves using $^{13}C/^{12}C$ isotope labeling. Plant Physiology **136,** 3245–3254.

O'Leary MH. 1988. Carbon isotopes in photosynthesis. Bioscience **38,** 328–336.

Parys E, Jastrzębski H. 2008. Mitochondria from leaf mesophyll cells of C_4 plants are deficient in the H protein of glycine decarboxylase complex. Journal of Plant Physiology **165,** 1061–1069.

Peterhansel C, Blume C, Offermann S. 2013*a*. Photorespiratory bypasses: how can they work? Journal of Experimental Botany **64,** 709–715.

Peterhansel C, Horst I, Niessen M, Blume C, Kebeish R, Kürkcüoglu S, Kreuzaler F. 2010. Photorespiration. The Arabidopsis Book **8,** e0130.

Peterhansel C, Krause K, Braun HP, Espie GS, Fernie AR, Hanson DT, Keech O, Maurino VG, Mielewczik M, Sage RF. 2013*b*. Engineering photorespiration: current state and future possibilities. Plant Biology **15,** 754–758.

Priault P, Wegener F, Werner C. 2009. Pronounced differences in diurnal variation of carbon isotope composition of leaf respired CO_2 among functional groups. New Phytologist **181,** 400–412.

Rademacher T, Häusler RE, Hirsch HJ, Zhang L, Lipka V, Weier D, Kreuzaler F, Peterhänsel C. 2002. An engineered phospho*enol*pyruvate carboxylase redirects carbon and nitrogen flow in transgenic potato plants. The Plant Journal **32,** 25–39.

Rooney MA. 1988. Short-term carbon isotopic fractionation in plants. PhD thesis, University of Wisconsin, Madison, WI, USA.

Sharkey TD, Berry JA, Raschke K. 1985. Starch and sucrose synthesis in *Phaseolus vulgaris* as affected by light, CO_2, and abscisic acid. Plant Physiology **77,** 617–620.

Somerville CR. 2001. An early *Arabidopsis* demonstration. Resolving a few issues concerning photorespiration. Plant Physiology **125,** 20–24.

Somerville CR, Ogren WL. 1982. Genetic modification of photorespiration. Trends in Biochemical Sciences **7,** 171–174.

Sonawane BV, Cousins AB. 2019. Uncertainties and limitations of using carbon-13 and oxygen-18 leaf isotope exchange to estimate the temperature response of mesophyll CO_2 conductance in C_3 plants. New Phytologist **222**, 122–131.

Stutz SS, Edwards GE, Cousins AB. 2014. Single-cell C_4 photosynthesis: efficiency and acclimation of *Bienertia sinuspersici* to growth under low light. New Phytologist **202,** 220–232.

Sun W, Ubierna N, Ma JY, Walker BJ, Kramer DM, Cousins AB. 2014. The coordination of C_4 photosynthesis and the CO_2-concentrating mechanism in maize and *Miscanthus* × *giganteus* in response to transient changes in light quality. Plant Physiology **164,** 1283–1292.

Tazoe Y, von Caemmerer S, Estavillo GM, Evans JR. 2011. Using tunable diode laser spectroscopy to measure carbon isotope discrimination and mesophyll conductance to CO_2 diffusion dynamically at different CO_2 concentrations. Plant, Cell & Environment **34,** 580–591.

Tcherkez G. 2006. How large is the carbon isotope fractionation of the photorespiratory enzyme glycine decarboxylase? Functional Plant Biology **33,** 911–920.

Tcherkez G, Bligny R, Gout E, Mahe´ A, Hodges M, Cornic G. 2008. Respiratory metabolism of illuminated leaves depends on CO_2 and O_2 conditions. Proceedings of the National Academy of Sciences, USA **105,** 797–802.

Tcherkez G, Boex-Fontvieille E, Mahé A, Hodges M. 2012. Respiratory carbon fluxes in leaves. Current Opinion in Plant Biology **15,** 308–314.

Tcherkez G, Cornic G, Bligny R, Gout E, Ghashghaie J. 2005. In vivo respiratory metabolism of illuminated leaves. Plant Physiology **138,** 1596–1606.

Tcherkez G, Farquhar GD, Badeck F, Ghashghaie J. 2004. Theoretical considerations about carbon isotope distribution in glucose of C_3 plants. Functional Plant Biology **31,** 857–877.

Tcherkez G, Nogués S, Bleton J, Cornic G, Badeck F, Ghashghaie J. 2003. Metabolic origin of carbon isotope composition of leaf dark-respired CO_2 in French bean. Plant Physiology **131,** 237–244.

Tcherkez G, Schäufele R, Nogués S, *et al*. 2010. On the $^{13}C/^{12}C$ isotopic signal of day and night respiration at the mesocosm level. Plant, Cell & Environment **33,** 900–913.

Timm S, Bauwe H. 2013. The variety of photorespiratory phenotypes—employing the current status for future research directions on photorespiration. Plant Biology **15,** 737–747.

Timm S, Florian A, Arrivault S, Stitt M, Fernie AR, Bauwe H. 2012. Glycine decarboxylase controls photosynthesis and plant growth. FEBS Letters **586,** 3692–3697.

Timm S, Giese J, Engel N, Wittmiß M, Florian A, Fernie AR, Bauwe H. 2018. T-protein is present in large excess over the other proteins of the glycine cleavage system in leaves of *Arabidopsis*. Planta **247,** 41–51.

Timm S, Nunes-Nesi A, Pärnik T, Morgenthal K, Wienkoop S, Keerberg O, Weckwerth W, Kleczkowski LA, Fernie AR, Bauwe H. 2008. A cytosolic pathway for the conversion of hydroxypyruvate to glycerate during photorespiration in *Arabidopsis*. The Plant Cell **20,** 2848–2859.

Ubierna N, Farquhar GD. 2014. Advances in measurements and models of photosynthetic carbon isotope discrimination in C_3 plants. Plant, Cell & Environment **37,** 1494–1498.

Ubierna N, Gandin A, Boyd RA, Cousins AB. 2017. Temperature response of mesophyll conductance in three C_4 species calculated with two methods: ^{18}O discrimination and *in vitro* V_{pmax}. New Phytologist **214,** 66–80.

Ubierna N, Sun W, Cousins AB. 2011. The efficiency of C_4 photosynthesis under low light conditions: assumptions and calculations with CO_2 isotope discrimination. Journal of Experimental Botany **62,** 3119–3134.

von Caemmerer S. 2000. Biochemical models of leaf photosynthesis. No. 2. Collingwood, Australia: CSIRO Publishing.

von Caemmerer S, Evans JR. 1991. Determination of the average partial pressure of CO_2 in chloroplasts from leaves of severa1 C_3 plants. Australian Journal of Plant Physiology **18,** 287–305.

von Caemmerer S, Ghannoum O, Pengelly JJ, Cousins AB. 2014. Carbon isotope discrimination as a tool to explore C_4 photosynthesis. Journal of Experimental Botany **65,** 3459–3470.

Walker BJ, Cousins AB. 2013. Influence of temperature on measurements of the CO_2 compensation point: differences between the Laisk and O_2-exchange methods. Journal of Experimental Botany **64,** 1893–1905.

Walker BJ, VanLoocke A, Bernacchi CJ, Ort DR. 2016. The costs of photorespiration to food production now and in the future. Annual Review of Plant Biology **67,** 107–129.

Werner C, Gessler A. 2011. Diel variations in the carbon isotope composition of respired CO_2 and associated carbon sources: a review of dynamics and mechanisms. Biogeosciences **8,** 2437–2459.

Werner C, Wegener F, Unger S, Nogués S, Priault P. 2009. Short-term dynamics of isotopic composition of leaf-respired CO_2 upon darkening: measurements and implications. Rapid Communications in Mass Spectrometry **23,** 2428–2438.

Wingler A, Lea PJ, Leegood RC. 1997. Control of photosynthesis in barley plants with reduced activities of glycine decarboxylase. Planta **202,** 171–178.

Wingler A, Lea PJ, Leegood RC. 1999. Photorespiratory metabolism of glyoxylate and formate in glycine**-**accumulating mutants of barley and *Amaranthus edulis*. Planta **207,** 518–526.

Wingler A, Lea PJ, Quick WP, Leegood RC. 2000. Photorespiration: metabolic pathways and their role in stress protection. Philosophical Transactions of the Royal Society B: Biological Sciences **355,** 1517–1529.